



Available online at [www.sciencedirect.com](http://www.sciencedirect.com)

**ScienceDirect**

[Geochimica et Cosmochimica Acta 141 \(2014\) 532–546](#)

**Geochimica et  
Cosmochimica  
Acta**

[www.elsevier.com/locate/gca](http://www.elsevier.com/locate/gca)

# Stable isotope records of hydrologic change and paleotemperature from smectite in Cenozoic western North America

Hari T. Mix <sup>\*</sup>, C. Page Chamberlain

*Department of Environmental Earth System Science, Stanford University, Stanford, CA 94305, USA*

Received 16 August 2013; accepted in revised form 8 July 2014; Available online 18 July 2014

---

## Abstract

The oxygen and hydrogen isotopic composition of soil water ( $\delta^{18}\text{O}_w$  and  $\delta\text{D}_w$  hereafter) reflect the history of water through processes such as source evaporation, precipitation and vapor recycling. Temperature, humidity, evaporation, and post-condensation processes can affect  $\delta^{18}\text{O}_w$  and  $\delta\text{D}_w$ . As such, isotope proxy records are often limited in their ability to constrain paleoclimate, paleoecology or paleoelevation without independently corroborating data. Smectite preserves both the hydrogen and oxygen isotope signature of parent water, and therefore provides critical insight into meteoric water line relationships and paleotemperature. Here, we use *in situ* pedogenic smectite  $\delta^{18}\text{O}$  and  $\delta\text{D}$  records to characterize the evolution of the hydrologic cycle in Cenozoic western North America. We incorporate 192 samples, 119 of which are previously unpublished, from 11 Cenozoic basins representing a range of environments in the Basin and Range, Rocky Mountains and Great Plains. Our results indicate that the processes controlling smectite isotopic compositions vary both regionally and temporally. In some localities such as Oligocene to Pleistocene western Nebraska, change in temperature is the primary control on smectite isotopic composition. In other basins such as in Miocene Trapper Creek, ID, isotope values lie along the meteoric water line, suggesting change in meteoric water composition is responsible for the variation. In most basins, especially those in the Neogene Basin and Range, smectite line slope suggests either evaporation of previously meteoric water or a combination of change in paleotemperature and meteoric water composition. Smectite geothermometry suggests mineral formation temperatures of 30–40 °C in the Middle Miocene in the Rocky Mountains, Great Plains and Basin and Range, and a decrease of 10–15 °C since the Middle Miocene Climatic Optimum, consistent with clumped isotope and paleofloral temperature estimates.

© 2014 Elsevier Ltd. All rights reserved.

---

## 1. INTRODUCTION

The oxygen and hydrogen isotopic compositions of soil water ( $\delta^{18}\text{O}_w$  and  $\delta\text{D}_w$  hereafter) reflect the history of water as they are affected by processes such as source evaporation, precipitation and vapor recycling (e.g., [Craig, 1961](#);

[Craig and Gordon, 1965](#)). A variety of geochemical proxies such as calcium carbonate, silicates, hydrated volcanic glass, and mammalian tooth enamel record the isotopic signature of ancient water, and have been widely applied to interpret and constrain paleoclimatic and paleotopographic change in western North America (e.g., [Kohn et al., 2002](#); [Poage and Chamberlain, 2002](#); [Horton et al., 2004](#); [Mulch et al., 2006, 2007, 2008](#); [Mix et al., 2011, 2013](#)). Since many factors can affect  $\delta^{18}\text{O}_w$  and  $\delta\text{D}_w$ , isotope records are often limited in their ability to constrain paleoclimate, paleoecology or paleoelevation without independently

---

\* Corresponding author. Address: Department of Environmental Earth System Science, 473 Via Ortega, Stanford, CA 94305-4216, USA. Tel.: +1 (650) 353 0903.

E-mail address: [hmix@stanford.edu](mailto:hmix@stanford.edu) (H.T. Mix).

corroborating data. This is particularly true for studies of a single isotope system, as these techniques are unable to constrain critical features of the hydrologic regime such as local meteoric water line slope and evaporation.

Smectite, along with other clay minerals, chert, goethite, gibbsite and some other materials provide the advantage of recording both the hydrogen and oxygen isotopic signatures of parent water (e.g., Lawrence and Taylor, 1971, 1972; Yeh and Epstein, 1978; Yapp, 1987), but have been less frequently applied (Stern et al., 1997; Chamberlain and Poage, 2000; Takeuchi and Larson, 2005; Abruzzese et al., 2005; Sjostrom et al., 2006; Mulch et al., 2006). Smectite refers to a family of 2:1 clay minerals that typically form as weathering products of aluminosilicates. The Cenozoic stratigraphy of western North America is well suited to the use of smectite as a proxy due to its abundant silicic ashes that weather rapidly to smectite in the shallow subsurface (Stanley and Benson, 1979; Stanley and Faure, 1979). Furthermore, these spatially-extensive ashes have been well studied and provide high quality radiometric age control for paleoclimate reconstructions.

Herein, we incorporate pedogenic smectite samples from a range of environments in the Basin and Range, Rocky Mountains and Great Plains (Fig. 1). First, we apply a combined oxygen and hydrogen isotope approach to characterize meteoric water relationships in the past. We use the slope of  $\delta^{18}\text{O}$ – $\delta\text{D}$  data to distinguish among meteoric water composition, temperature, and/or aridity as drivers of isotopic change. Second, due to differences in the equilibrium fractionation of hydrogen and oxygen, the temperature of mineral formation can be reconstructed with smectite  $\delta^{18}\text{O}$  and  $\delta\text{D}$  values. In this study, we produce long-term temperature records from smectite in western North America. In short, our findings demonstrate that causes of isotopic change in smectite vary both spatially and temporally, and that mineral formation temperatures decreased since the Middle Miocene.

## 2. COMBINED OXYGEN AND HYDROGEN ISOTOPE APPROACH

### 2.1. $\delta^{18}\text{O}$ – $\delta\text{D}$ relationships in meteoric water and smectite

$\delta^{18}\text{O}$  and  $\delta\text{D}$  of meteoric water reflect many aspects of the hydrologic cycle, and have since been used in a number of applications including studies of paleoelevation, decoupling evaporation and transpiration and delineating air mass trajectories (Craig, 1961; Dansgaard, 1964; Rozanski et al., 1993). Globally, precipitation falls on a meteoric water line (GMWL) with a slope of approximately 8, and a  $y$ -intercept, or deuterium excess, of approximately 10 (Friedman, 1953; Craig, 1961) (Fig. 2). Regional variations in these slopes and intercepts in meteoric and surface waters are large, however. In the continental United States, the slopes of local meteoric water lines (LMWLs) inferred from stream waters range from 5 to 13, with an average of 6.1 (Kendall and Coplen, 2001). LMWL slopes are often lower than the GMWL value of ~8 due to low humidity and evaporation (Yurtsever and Gat, 1981). This relationship reflects differences in the kinetic effects of oxygen and hydrogen associated with evaporation, driving waters to evolve along an evaporation trend of a lower slope than the GMWL. The slope decreases as relative humidity decreases. For example, in arid environments with relative humidity less than 25%, surface water line slopes are ~4, whereas for a relative humidity of over 95%, the evaporation-driven trend approaches the GMWL slope of ~8 (Clark and Fritz, 1997). Smectite that forms in equilibrium with these waters will create linear arrays on  $\delta^{18}\text{O}$ – $\delta\text{D}$  diagrams, hereafter referred to as *smectite lines*. The gap between the smectite lines and the meteoric water line represent the temperature-dependent equilibrium fractionation between smectite and water (Fig. 2).

For each stratigraphic section included in this study, we plotted  $\delta^{18}\text{O}$  vs.  $\delta\text{D}$  in order to examine the relationships

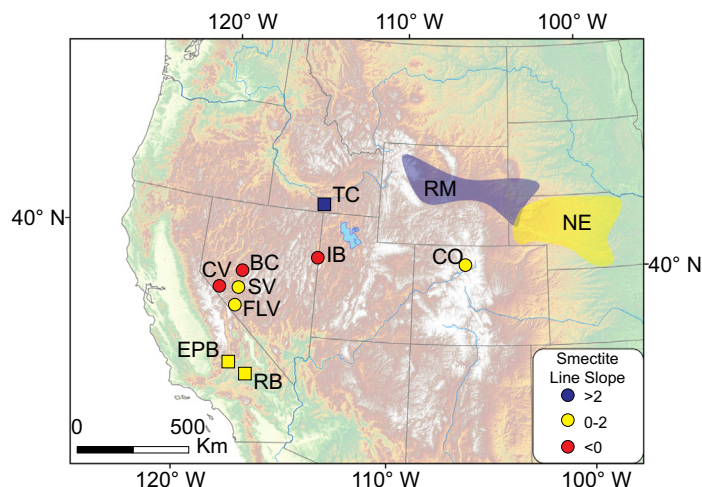


Fig. 1. The eleven stratigraphic sections used in this study. Circles indicate new data while squares show previously published work. Color represents ancient meteoric water line slope reconstructed from smectite. The two shaded regions show the sampled area for composite sections of the east-flank of the Rocky Mountains of Sjostrom et al. (2006) and Nebraska (this study). (For interpretation of the references to color in this figure legend, the reader is referred to the web version of this article.)

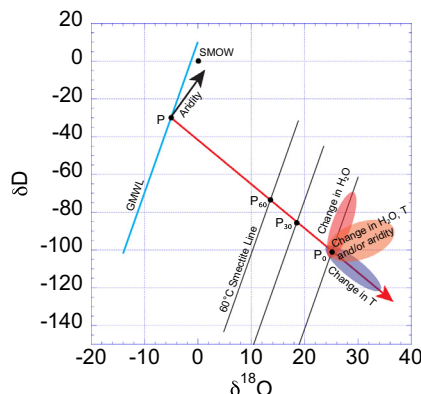


Fig. 2. Isotopic relationships between meteoric water and smectite. GMWL: Global meteoric water line displayed in blue. SMOW: Standard mean ocean water. Smectite lines parallel to the GMWL at 60, 30 and 0 °C are drawn. Red line indicates change in mineral formation temperature. (For interpretation of the references to color in this figure legend, the reader is referred to the web version of this article.)

among the trends of meteoric waters, temperature, and evaporation. A smectite line parallel to the modern GMWL was fit through  $\delta^{18}\text{O}$ – $\delta\text{D}$  data from each basin. We used smectite– $\text{H}_2\text{O}$  fractionation factors for oxygen (Sheppard and Gilg, 1996) and hydrogen (Capuano, 1992) to convert from meteoric water values to equivalent smectite  $\delta^{18}\text{O}$  and  $\delta\text{D}$  values using the average isotope-based temperature calculated (See Section 4.2). In addition, we plotted temperature trendlines by using the average mineral  $\delta^{18}\text{O}$  and  $\delta\text{D}$  values and a range of temperature inputs into the appropriate fractionation equations. As evaporative environments can encompass a range of potential smectite line slopes, the slope of mineral  $\delta^{18}\text{O}$  vs.  $\delta\text{D}$  values was used to assess relative humidity and degree of evaporation.

## 2.2. Stable isotope-based geothermometry of smectite

Oxygen isotopic fractionation factors in most mineral–water systems are positive at natural surface temperatures, such that the mineral becomes enriched in  $^{18}\text{O}$  relative to water at a given temperature. In contrast, hydrogen isotope fractionation factors in many sheet silicates are negative, such that the mineral is depleted in deuterium with respect to water. This depletion increases with an increase in temperature (Yeh, 1980; Capuano, 1992). These differing fractionation properties allows for the calculation of the temperature of smectite formation if given its  $\delta^{18}\text{O}$  and  $\delta\text{D}$  values (Delgado and Reyes, 1996).

Here we calculate temperatures of smectite formation following the method of Delgado and Reyes (1996). We follow the same line of reasoning and use the hydrogen isotopic fractionation factor of Capuano (1992), the oxygen isotopic fractionation factor of Savin and Lee (1988), and assume the smectites form in equilibrium with waters along the GMWL. Although this model was originally validated through studies of Tertiary bentonites, it has since been applied in several studies including those: (1) of Mesozoic

and Paleozoic paleosols (Vitali et al., 2002; Tabor et al., 2004; Tabor and Montañez, 2005; Myers et al., 2011) and (2) of secondary smectite formed in an impact crater (Muttik et al., 2010). The error associated with these paleotemperatures is about  $\pm 3$  °C (Tabor and Montañez, 2005), which is slightly greater than the  $\pm 1.2$ – $2.4$  °C precision currently reported for the carbonate clumped isotope method (Huntington et al., 2009).

## 3. METHODS

### 3.1. Sampling and preparation of smectite

During 2008, 2009 and 2010, we collected samples of volcanic ash from seven basins in western North America. In the Basin and Range, we sampled the principal sections of the Miocene Wassuk Group in Coal Valley, NV; the Miocene Stewart Valley Group in Stewart Valley, NV; the Miocene Buffalo Canyon Formation in Buffalo Canyon, NV; the Miocene to Pleistocene sediments of Fish Lake Valley, NV; and the Miocene Salt Lake Formation in the Ibapah Badlands, UT (Heylmun, 1965; Golia and Stewart, 1984; Schorn et al., 1989; Axelrod, 1991; Reheis and Sawyer, 1997; Perkins et al., 1998; Reheis and Block, 2007). In the Rocky Mountains, we sampled the Miocene Troublesome, North Park, and Browns Park Formations in the Middle and North Park Basins, CO (Beekly, 1915; Montagne and Barnes, 1957; Izett, 1968; Izett and Barclay, 1973; Montagne, 1991). In Nebraska, we produced a composite section of isotopic data from the Miocene Ari-karee and Hemingford Groups, the Pliocene Ogallala Group, and several younger Tertiary and Quaternary ashes (Swineford et al., 1955; Stout et al., 1971; Boellstorff, 1976; Swinehart et al., 1985; Diffendal, 1995). Additionally, we incorporated published isotopic records from several regions: (1) Miocene sediments in the Carlin-Piñon Range, Virgin Valley, and Willow Creek, NV, Rash Valley, UT, Trapper Creek, ID and Pliocene sediments near Oreana, ID (Horton et al., 2004); (2) The Miocene Rainbow and El Paso Basins, CA (Horton and Chamberlain, 2006); and (3) Eocene to Miocene volcanic ashes from Nebraska, South Dakota and Wyoming (Sjostrom et al., 2006).

In order to isolate authigenic smectite, bulk samples of volcanic ash were broken, ground, or blended (if necessary) until disaggregated. Approximately 200 g of this material was suspended in deionized water, after which the  $<0.5 \mu\text{m}$  size fraction was isolated with a Thermo IEC centrifuge to remove non-smectite clays and other minerals. Samples were confirmed to be smectite through X-ray diffraction analysis. Following the methods of Moore and Reynolds (1997), samples were mounted and air-dried on glass slides. Samples were subject to X-ray diffraction analysis using a PANalytical X'Pert PRO Materials Research Diffractometer configured with mirror and parallel plate collimator optics in the Stanford Nanocharacterization Laboratory. The samples were then analyzed before and after ethylene glycol solvation. A shift in the  $001$  reflection from  $6^\circ 2\theta$  in the air-dried state to  $5.2^\circ 2\theta$  following glycolation was considered diagnostic of smectite (Moore and Reynolds, 1997).

### 3.2. Stable isotope analysis

Stable isotope analysis of authigenic smectite were performed at the Stable Isotope Biogeochemistry Laboratory at Stanford University following procedures similar to Sharp (1990) and Takeuchi and Larson (2005). Hydrogen isotopic composition was obtained through continuous flow mass spectrometry using a thermal combustion elemental analyzer coupled to a Thermo Finnigan DeltaPlusXL mass spectrometer. Samples were enclosed in silver foil, then placed in a Fisher Scientific Isotemp vacuum oven at 80 °C and –100 kPa pressure for at least 3 days before isotopic analysis. Samples were run with polyethylene foil, oil, and kaolinite standard materials. Instrumental error for this method is typically less than 2‰ in δD. Oxygen isotopic composition was determined using a laser fluorination line coupled to a Thermo Finnigan MAT 252 mass spectrometer in a dual inlet configuration. Samples were physically mixed with LiF, then pressed into a pellet to prevent dispersion during lasing, then isolated in a vacuum oven as mentioned above. Samples were subjected to three 90-s exposures to BrF<sub>5</sub> in order to liberate excess water and impurities from the samples and fluorination line. Samples were then reacted with BrF<sub>5</sub> and heated using a New Wave Research MIR10–25 infrared laser ablation system, liberating O<sub>2</sub> gas. The oxygen gas was purified through several cold traps and a KBr trap before being introduced into the mass spectrometer. Repeated analysis of quartz, garnet and smectite standards have shown the precision of this method to be <0.2‰ in δ<sup>18</sup>O. All isotopic ratios are reported relative to Vienna Standard Mean Ocean Water (V-SMOW).

### 3.3. Elemental analysis

Elemental analysis was performed by the Peter Hooper GeoAnalytical Lab at the Washington State University School of the Environment. Five samples were ground to a powder finer than 50 µm, mixed with di-lithium tetraborate flux (2:1 flux:rock) and fused at 1000 °C. Samples were then reground, refused and polished on diamond laps before elemental analysis using a ThermoARL Advant'XP sequential X-ray fluorescence spectrometer. The preparatory and analysis procedures follow the work of Johnson et al. (1999). Chemical formulae were calculated using XRF oxide data and based on twelve oxygen and two hydrogen atoms per unit cell (Moore and Reynolds, 1997).

## 4. RESULTS

### 4.1. Characterization of δ<sup>18</sup>O vs. δD arrays for smectite

We used our isotopic records to examine the state of ancient hydrologic regimes by plotting δ<sup>18</sup>O vs. δD for each stratigraphic section. The slope of the δ<sup>18</sup>O and δD data varied widely from basin to basin (Fig. 3). The Buffalo Canyon, Ibapah Badlands, and Coal Valley sections all showed a negative slopes. The sections in Nebraska, Middle and North Park, Stewart Valley, Rainbow Basin, El Paso Basin, and Fish Lake Valley have low but positive slopes ranging

from 0.3 to 1.1. Finally, the Eocene to Miocene eastern flank of the Rocky Mountains and Trapper Creek, ID exhibit large positive slopes of 2.3 and 5.4, respectively.

### 4.2. Smectite geothermometry

We calculated isotope-based temperatures for each smectite sample. First, we observe that Neogene smectite temperatures vary substantially by region (Table 1). The coolest temperatures observed are in Nebraska, with a mean of 13.2 ± 5.7 °C. The warmest temperatures are in Coal Valley, NV and Trapper Creek, ID, with means of 40.2 ± 7.9 and 43.2 ± 4.3 °C, respectively. The remaining sections from the Neogene Basin and Range and the Paleogene east-flank of the Rocky Mountains have mean smectite temperatures ranging from 26.6 to 35.2 °C.

Second, we plotted temperature records for each major section (Fig. 4). In the Middle to Late Miocene El Paso Basin (CA), the results of a two-tailed heteroscedastic *t*-test indicates decreasing mineral formation temperatures (*p* = 0.02). Temperatures in Middle to Late Miocene Coal Valley (NV), however, increase (*p* = 0.03). In most basins, however, we lack a sufficient number of samples to resolve if any perceived temperature trends are statistically significant. In order to assess prevailing regional trends, we produced composite temperature records for the Basin and Range as well as the Rocky Mountain/Great Plains regions (Fig. 5). A composite record consisting of binned data in the Basin and Range shows decreasing smectite temperatures throughout Neogene time, from over 40 °C in the Early to Middle Miocene to under 25 °C by the Quaternary. In the Rocky Mountains and Great Plains, temperatures from the Eocene until the Early Miocene range between 27 and 34 °C, and increase to 39 °C in the Middle Miocene. Temperatures then decrease to under 20 °C since the Middle Miocene. Two-tailed heteroscedastic *t*-tests confirmed that cooling between the Middle Miocene and Pleistocene was statistically significant (Basin and Range *p* = 0.02, Rocky Mountains and Great Plains *p* = 3 × 10<sup>−5</sup>).

## 5. DISCUSSION

We interpret the long-term smectite record presented here in the context of paleoenvironmental change. Our δ<sup>18</sup>O–δD results demonstrate multiple controls on smectite isotopic composition and smectite geothermometry documents the long-term climatic cooling of western North America since the Middle Miocene.

### 5.1. Characterization of meteoric water relationships in Neogene western North America

Our results indicate that the processes controlling smectite δ<sup>18</sup>O and δD vary both regionally and temporally. We observe great differences in smectite line slopes from basin to basin, which we infer to reflect multiple controls on isotopic composition (Fig. 1). The basins with the highest smectite line slopes are in Middle Miocene Trapper Creek, ID (5.4) and the Eocene to Miocene east-

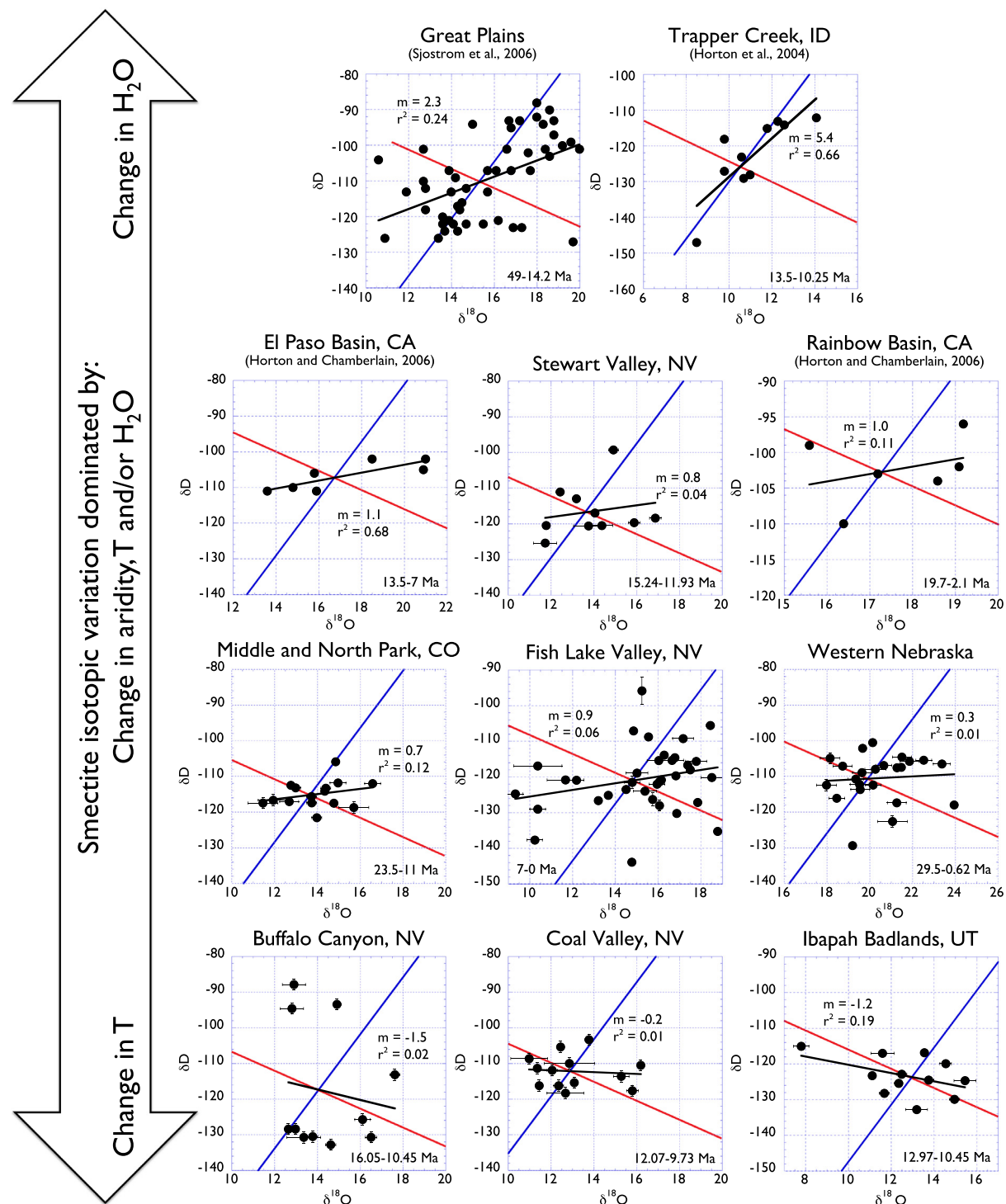


Fig. 3. Meteoric water relationships from Cenozoic basins in western North America. Blue lines are a smectite line parallel to the global meteoric water line. Red lines represent variation in temperature with no variation in isotopic composition of meteoric water. Black lines are linear regressions of smectite  $\delta^{18}\text{O}$ - $\delta\text{D}$  data. (For interpretation of the references to color in this figure legend, the reader is referred to the web version of this article.)

Table 1

Isotope and temperature records used in this study with relevant references. Temperatures were calculated using the global meteoric water relationship of  $\delta D = 8\delta^{18}\text{O} + 10$  (Craig, 1961) and the following smectite-water fractionation factors:  $10^3 \ln \alpha_{\text{ox}} = 2.60 (10^6 T^{-2}) - 4.28$  (Savin and Lee, 1988);  $10^3 \ln \alpha_{\text{hy}} = -45.3 (10^3 T^{-1}) + 94.7$  (Capuano, 1992).

Sample	Latitude	Longitude	Age (Ma)	$\delta^{18}\text{O}$	$1\sigma$	$\delta D$	$1\sigma$	Temperature (°C)	Key references
<i>Middle and North Park, CO</i>									
HM09-CO1	40.0813	-106.3725	11.00	14.78	0.02	-117.58	0.45	30.4	Montagne and Barnes (1957), Izett (1968)
HM09-CO2	40.0813	-106.3725	11.00	16.59	0.37	-112.08	0.45	26.0	Montagne and Barnes (1957), Izett (1968)
HM09-CO3	40.0813	-106.3725	11.00	13.98	0.23	-121.67	0.45	31.5	Montagne and Barnes (1957), Izett (1968)
HM10-CO12	40.6681	-106.4117	13.40	11.46	0.7	-117.56	1.57	44.4	Montagne and Barnes (1957), Izett (1968)
HM10-CO7	40.6696	-106.4288	13.50	15.71	0.7	-118.81	1.57	26.2	Montagne and Barnes (1957), Izett (1968)
HM09-CO11	40.0297	-106.3021	15.20	13.74	0.23	-117.51	0.45	34.6	Montagne and Barnes (1957), Izett (1968)
HM09-CO10	40.0281	-106.3022	16.50	12.99	0.23	-113.29	0.45	40.0	Montagne and Barnes (1957), Izett (1968)
HM09-CO9	40.0249	-106.3058	17.00	14.86	0.02	-105.97	0.45	35.9	Montagne and Barnes (1957), Izett (1968)
HM10-CO1	40.6719	-106.4143	17.00	11.94	0.7	-116.76	1.57	42.7	Montagne and Barnes (1957), Izett (1968)
HM09-CO8	40.0249	-106.3058	17.10	14.40	0.23	-113.39	0.45	34.0	Montagne and Barnes (1957), Izett (1968)
HM09-CO7	40.0249	-106.3058	18.90	14.35	0.02	-114.23	0.45	33.8	Montagne and Barnes (1957), Izett (1968)
HM09-CO12	40.0249	-106.3058	18.90	12.69	0.44	-117.14	0.45	39.2	Montagne and Barnes (1957), Izett (1968)
HM09-CO6	40.0249	-106.3058	19.00	14.97	0.37	-111.92	0.45	32.4	Montagne and Barnes (1957), Izett (1968)
HM09-CO4	40.0033	-106.3401	23.00	13.73	0.23	-115.73	0.45	35.6	Montagne and Barnes (1957), Izett (1968)
HM09-CO5	40.0033	-106.3401	23.50	12.77	0.02	-112.57	0.45	41.3	Montagne and Barnes (1957), Izett (1968)
Mean	40.1628	-106.3457		13.9		-115.1		35.2	
<i>Nebraska</i>									
HM10-NE10	40.7265	-100.3041	0.62	18.00	0.46	-112.54	1.57	20.6	Stout et al. (1971)
HM10-NE11	40.6425	-100.0809	0.62	18.17	0.46	-104.99	1.57	23.5	Stout et al. (1971)
HM09-NE24	40.1887	-98.1722	0.76	21.50	0.17	-107.53	0.84	10.9	Stout et al. (1971)
HM09-NE25	40.1964	-98.1828	0.76	20.16	0.02	-100.60	0.84	18.3	Stout et al. (1971)
HM09-NE21	42.8377	-100.5199	2.30	21.88	0.44	-105.86	0.84	10.3	Boellstorff (1976)
HM09-NE23	41.3863	-99.0605	2.30	19.69	0.02	-102.19	0.84	19.2	Stout et al. (1971)
HM09-NE22	42.7953	-97.8666	5.00	21.53	0.44	-104.65	0.84	11.9	Boellstorff (1976)
HM09-NE6	41.2522	-102.1300	6.80	19.55	0.44	-112.31	0.84	15.3	Boellstorff (1976)
HM09-NE7	41.2522	-102.1300	6.80	18.76	0.44	-107.19	0.84	20.3	Boellstorff (1976)
HM09-NE8	41.4454	-102.9830	7.00	23.97	0.02	-118.08	0.84	-0.7	Boellstorff (1976)
HM09-NE3	41.1385	-101.6780	7.60	20.18	0.37	-112.51	0.84	13.1	Boellstorff (1976)
HM09-NE4	41.2620	-102.1069	8.00	19.22	0.02	-129.50	0.84	9.3	Boellstorff (1976)
HM09-NE5	41.2620	-102.1069	8.00	19.66	0.44	-109.01	0.84	16.4	Boellstorff (1976)
HM09-NE1	41.1831	-103.0674	8.20	21.29	0.44	-117.49	0.84	7.6	Boellstorff (1976)
HM09-NE2	41.1831	-103.0674	8.20	19.37	0.37	-110.84	0.84	16.6	Boellstorff (1976)
HM09-NE9	41.4564	-103.0534	8.50	19.58	0.44	-113.76	0.84	14.6	Boellstorff (1976)
HM10-NE3	41.4867	-102.8624	8.50	21.09	0.7	-122.74	1.57	6.2	Diffendal (1995)
HM09-NE20	42.6756	-100.8557	10.60	22.55	0.37	-105.54	0.84	8.3	Boellstorff (1976)
HM09-NE14	42.1965	-103.7873	16.00	20.68	0.37	-107.01	0.84	13.7	Swineford et al. (1955)
HM09-NE18	42.4956	-102.7988	16.00	23.40	0.40	-106.60	0.84	5.2	Swineford et al. (1955)
HM09-NE15	42.1965	-103.7873	16.50	20.29	0.49	-108.07	0.84	14.6	Swineford et al. (1955)
HM09-NE19	42.4956	-102.7988	17.00	21.30	0.12	-107.65	0.84	11.4	Swineford et al. (1955)
HM09-NE13	41.7000	-103.3466	29.50	18.48	0.37	-116.22	0.84	17.3	Swineford et al. (1955)
Mean	41.5415	-101.5977		20.4		-110.6		13.2	
<i>Fish Lake Valley, NV</i>									
HM08-WW26	37.3821	-117.7929	0.75	15.57	0.09	-108.84	0.32	31.6	Reheis and Sawyer (1997), Reheis and Block (2007)
HM08-WW25	37.3779	-117.7951	1.25	13.69	0.09	-125.23	0.32	30.9	Reheis and Sawyer (1997), Reheis and Block (2007)
HM08-WW24	37.3780	-117.7949	1.50	16.08	0.09	-121.41	0.32	23.6	Reheis and Sawyer (1997), Reheis and Block (2007)
HM08-WW23	37.3777	-117.7944	2.00	18.53	0.51	-120.22	0.32	15.4	Reheis and Sawyer (1997), Reheis and Block (2007)
HM08-WW22	37.3717	-117.7960	2.25	18.80	0.07	-135.37	0.32	8.4	Reheis and Sawyer (1997), Reheis and Block (2007)
HM08-WW21	37.3703	-117.7958	2.50	10.39	0.36	-129.13	0.32	42.7	Reheis and Sawyer (1997), Reheis and Block (2007)
HM08-WW19	37.3768	-117.7906	3.25	10.25	0.36	-137.80	0.32	38.6	Reheis and Sawyer (1997), Reheis and Block (2007)

Table 1 (continued)

Sample	Latitude	Longitude	Age (Ma)	$\delta^{18}\text{O}$	1 $\sigma$	$\delta\text{D}$	1 $\sigma$	Temperature (°C)	Key references
HM08-WW20	37.3698	-117.7954	3.25	11.69	0.86	-120.93	0.32	41.5	Reheis and Sawyer (1997), Reheis and Block (2007)
HM08-WW1	37.3670	-117.7923	3.40	10.39	1.13	-116.98	0.32	49.7	Reheis and Sawyer (1997), Reheis and Block (2007)
HM08-WW2	37.3670	-117.7923	3.50	15.97	0.36	-122.12	0.32	23.7	Reheis and Sawyer (1997), Reheis and Block (2007)
HM08-WW17	37.3700	-117.7883	4.00	16.85	0.12	-119.77	0.32	21.5	Reheis and Sawyer (1997), Reheis and Block (2007)
HM08-WW18	37.3702	-117.7918	4.00	17.19	0.49	-109.32	0.32	25.1	Reheis and Sawyer (1997), Reheis and Block (2007)
HM08-WW3	37.3670	-117.7922	4.25	14.52	0.19	-123.59	0.32	28.4	Reheis and Sawyer (1997), Reheis and Block (2007)
HM08-WW16	37.3690	-117.7885	4.50	14.79	0.17	-143.97	0.32	18.1	Reheis and Sawyer (1997), Reheis and Block (2007)
HM08-WW13	37.3686	-117.7885	4.75	13.22	0.09	-126.71	0.32	32.0	Reheis and Sawyer (1997), Reheis and Block (2007)
HM08-WW14	37.3686	-117.7885	4.75	15.03	0.51	-118.97	0.32	28.7	Reheis and Sawyer (1997), Reheis and Block (2007)
HM08-WW15	37.3686	-117.7885	4.75	18.46	0.19	-105.61	0.32	22.1	Reheis and Sawyer (1997), Reheis and Block (2007)
HM08-WW4	37.3669	-117.7921	5.00	12.20	0.09	-120.97	0.32	39.2	Reheis and Sawyer (1997), Reheis and Block (2007)
HM08-WW5	37.3669	-117.7921	5.00	16.17	0.09	-120.93	0.32	23.5	Reheis and Sawyer (1997), Reheis and Block (2007)
HM08-WW9	37.3669	-117.7863	5.00	17.52	0.17	-118.07	0.32	19.9	Reheis and Sawyer (1997), Reheis and Block (2007)
HM08-WW10	37.3669	-117.7863	5.00	16.30	0.09	-113.94	0.32	26.3	Reheis and Sawyer (1997), Reheis and Block (2007)
HM08-WW11	37.3674	-117.7864	5.00	14.87	0.01	-107.16	0.32	35.3	Reheis and Sawyer (1997), Reheis and Block (2007)
HM08-WW12	37.3674	-117.7864	5.00	9.34	0.36	-124.83	0.32	50.0	Reheis and Sawyer (1997), Reheis and Block (2007)
HM08-WW6	37.3669	-117.7921	5.20	16.05	0.54	-115.48	0.32	26.5	Reheis and Sawyer (1997), Reheis and Block (2007)
HM08-HT9	37.3421	-117.8410	5.75	15.40	0.54	-124.07	0.32	24.9	Reheis and Sawyer (1997), Reheis and Block (2007)
HM08-HT6	37.3429	-117.8404	6.50	17.40	0.17	-116.77	0.32	20.9	Reheis and Sawyer (1997), Reheis and Block (2007)
HM08-HT7	37.3429	-117.8404	6.50	17.80	0.49	-115.70	0.32	19.9	Reheis and Sawyer (1997), Reheis and Block (2007)
HM08-HT5	37.3436	-117.8401	6.75	16.80	0.09	-114.67	0.32	24.0	Reheis and Sawyer (1997), Reheis and Block (2007)
HM08-HT4	37.3438	-117.8399	7.00	16.67	0.54	-115.42	0.32	24.2	Reheis and Sawyer (1997), Reheis and Block (2007)
HM08-CSW7	37.8518	-117.9917	0.00	14.81	0.36	-121.6	1.8	28.3	Reheis and Sawyer (1997), Reheis and Block (2007)
HM08-CSW6	37.8373	-117.9171	1.05	16.89	0.12	-130.33	0.32	16.7	Reheis and Sawyer (1997), Reheis and Block (2007)
HM08-CSW4	37.8339	-117.9058	1.80	17.87	0.07	-127.23	0.32	14.7	Reheis and Sawyer (1997), Reheis and Block (2007)
HM08-CSW1	37.8246	-117.8868	5.00	15.76	0.12	-126.4	1.8	22.5	Reheis and Sawyer (1997), Reheis and Block (2007)
HM08-CSW2	37.8246	-117.8868	5.00	15.26	0.17	-95.9	3.8	39.6	Reheis and Sawyer (1997), Reheis and Block (2007)
HM08-CSW3	37.8246	-117.8868	5.00	16.08	0.01	-128.10	1.57	20.5	Reheis and Sawyer (1997), Reheis and Block (2007)
Mean	37.4458	-117.8190		15.3		-120.7		27.4	
<i>Stewart Valley, NV</i>									
HM08-SV1	38.5547	-117.9392	11.93	14.39	0.51	-120.50	0.84	30.4	Schorn et al. (1989), Perkins et al. (1998)
HM08-SV4	38.5549	-117.9512	12.02	11.74	0.54	-125.40	0.84	38.9	Schorn et al. (1989), Perkins et al. (1998)
HM08-SV5	38.5549	-117.9505	12.07	14.93	0.23	-99.25	0.84	39.2	Schorn et al. (1989), Perkins et al. (1998)
HM08-SV6	38.5544	-117.9500	12.96	13.20	0.07	-112.94	0.84	39.3	Schorn et al. (1989), Perkins et al. (1998)
HM08-SV7	38.5542	-117.9501	12.97	13.77	0.70	-120.58	0.84	32.9	Schorn et al. (1989), Perkins et al. (1998)
HM08-SV8	38.5536	-117.9481	13.73	15.90	0.27	-119.68	0.84	25.0	Schorn et al. (1989), Perkins et al. (1998)
HM08-SV9	38.5536	-117.9481	13.78	12.44	0.19	-111.06	0.84	43.6	Schorn et al. (1989), Perkins et al. (1998)
HM08-SV12	38.6083	-117.9406	14.93	11.79	0.09	-120.48	0.84	41.3	Schorn et al. (1989), Perkins et al. (1998)
HM08-SV2	38.5538	-117.9541	15.17	14.07	0.09	-116.95	0.84	33.5	Schorn et al. (1989), Perkins et al. (1998)
HM08-SV3	38.5538	-117.9540	15.24	16.89	0.27	-118.40	0.84	22.0	Schorn et al. (1989), Perkins et al. (1998)
Mean	38.5596	-117.9486		13.9		-116.5		34.6	
<i>Buffalo Canyon, NV</i>									
HM08-BC13	39.2581	-117.8392	10.45	12.98	0.07	-128.57	1.57	32.1	Axelrod (1991), Perkins et al. (1998)
HM08-BC12	39.2579	-117.8395	11.59	16.12	0.36	-125.91	1.57	21.4	Axelrod (1991), Perkins et al. (1998)
HM08-BC11	39.2579	-117.8395	11.80	17.63	0.24	-113.33	1.57	21.6	Axelrod (1991), Perkins et al. (1998)
HM08-BC10	39.2579	-117.8395	12.07	13.37	0.79	-130.92	1.57	29.3	Axelrod (1991), Perkins et al. (1998)
HM08-BC9	39.2117	-117.7940	15.17	14.63	0.24	-132.99	1.57	23.6	Axelrod (1991), Perkins et al. (1998)
HM08-BC8	39.2116	-117.7938	15.21	12.65	0.07	-128.59	1.57	33.4	Axelrod (1991), Perkins et al. (1998)
HM08-BC7	39.2114	-117.7938	15.24	16.52	0.27	-130.88	1.57	17.7	Axelrod (1991), Perkins et al. (1998)
HM08-BC6	39.2114	-117.7938	15.41	13.79	0.24	-130.69	1.57	27.8	Axelrod (1991), Perkins et al. (1998)

(continued on next page)

**Table 1** (continued)

Sample	Latitude	Longitude	Age (Ma)	$\delta^{18}\text{O}$	1 $\sigma$	$\delta\text{D}$	1 $\sigma$	Temperature (°C)	Key references
HM08-BC4	39.2012	-117.7918	15.84	12.82	0.54	-94.78	1.57	51.3	Axelrod (1991), Perkins et al. (1998)
HM08-BC3	39.2009	-117.7914	16.00	14.92	0.19	-93.59	1.57	42.3	Axelrod (1991), Perkins et al. (1998)
HM08-BC2	39.2009	-117.7914	16.05	12.91	0.54	-88.02	1.57	55.0	Axelrod (1991), Perkins et al. (1998)
Mean	39.2255	-117.8098		14.4		-118.0		32.3	
<i>Coal Valley, NV</i>									
HM08-CV15	38.5047	-118.9115	9.73	12.37	0.23	-116.43	1.57	41.0	Golia and Stewart (1984), Perkins et al. (1998)
HM08-CV13	38.5015	-118.9098	9.81	10.99	0.86	-108.83	1.57	51.7	Golia and Stewart (1984), Perkins et al. (1998)
HM08-CV14	38.5015	-118.9099	10.19	11.46	0.09	-116.41	1.57	45.1	Golia and Stewart (1984), Perkins et al. (1998)
HM08-CV11	38.4991	-118.9043	10.54	12.87	1.18	-110.18	1.57	42.2	Golia and Stewart (1984), Perkins et al. (1998)
HM08-CV8	38.4989	-118.9016	10.94	12.46	0.09	-105.55	1.57	46.7	Golia and Stewart (1984), Perkins et al. (1998)
HM08-CV9	38.4989	-118.9016	11.31	11.37	0.09	-111.53	1.57	48.3	Golia and Stewart (1984), Perkins et al. (1998)
HM08-CV10	38.4989	-118.9016	11.51	12.07	0.24	-112.10	1.57	44.7	Golia and Stewart (1984), Perkins et al. (1998)
HM08-CV7	38.4984	-118.9014	11.57	13.79	0.19	-103.51	1.57	41.8	Golia and Stewart (1984), Perkins et al. (1998)
HM08-CV4	38.4957	-118.8987	11.59	15.82	0.27	-117.84	1.57	26.2	Golia and Stewart (1984), Perkins et al. (1998)
HM08-CV5	38.4959	-118.8986	11.72	12.69	0.86	-118.51	1.57	38.5	Golia and Stewart (1984), Perkins et al. (1998)
HM08-CV2	38.4945	-118.8976	11.93	16.21	0.12	-110.69	1.57	28.2	Golia and Stewart (1984), Perkins et al. (1998)
HM08-CV3	38.4944	-118.8978	12.01	15.30	0.36	-113.80	1.57	30.2	Golia and Stewart (1984), Perkins et al. (1998)
HM08-CV1	38.4934	-118.8964	12.07	13.10	0.12	-115.57	1.57	38.3	Golia and Stewart (1984), Perkins et al. (1998)
Mean	38.4981	-118.9024		13.1		-112.4		40.2	
<i>Ibapah Badlands, UT</i>									
HM08-IB19	40.1104	-114.0757	10.45	14.99	0.24	-130.12	0.45	23.6	Heylmun (1965), Perkins et al. (1998)
HM08-IB18	40.1104	-114.0758	10.54	15.48	0.51	-124.89	0.45	24.2	Heylmun (1965), Perkins et al. (1998)
HM08-IB10	40.1122	-114.0838	11.72	11.14	0.17	-123.46	0.45	42.5	Heylmun (1965), Perkins et al. (1998)
HM08-IB21	40.1162	-114.0945	11.82	12.38	0.19	-125.63	0.45	36.0	Heylmun (1965), Perkins et al. (1998)
HM08-IB9	40.1288	-114.1725	12.01	13.78	0.24	-124.72	0.45	30.8	Heylmun (1965), Perkins et al. (1998)
HM08-IB8	40.1288	-114.1724	12.02	11.62	0.54	-117.21	0.45	43.9	Heylmun (1965), Perkins et al. (1998)
HM08-IB7	40.1288	-114.1722	12.07	11.71	0.24	-128.41	0.45	37.4	Heylmun (1965), Perkins et al. (1998)
HM08-IB6	40.1287	-114.1721	12.14	14.58	0.27	-120.13	0.45	29.9	Heylmun (1965), Perkins et al. (1998)
HM08-IB5	40.1289	-114.1720	12.34	13.58	0.12	-117.03	0.45	35.5	Heylmun (1965), Perkins et al. (1998)
HM08-IB3	40.1290	-114.1719	12.83	12.52	0.24	-123.05	0.45	36.8	Heylmun (1965), Perkins et al. (1998)
HM08-IB2	40.1289	-114.1717	12.84	13.22	0.51	-133.00	0.45	28.9	Heylmun (1965), Perkins et al. (1998)
HM08-IB1	40.1292	-114.1710	12.97	7.82	0.36	-115.25	0.45	63.8	Heylmun (1965), Perkins et al. (1998)
Mean	40.1233	-114.1421		12.7		-123.6		36.1	
<i>East Flank of the Rocky Mountains (Sjostrom et al., 2006)</i>									
01DS104	42.4460	-107.5316	14.2	15.7		-107		32.0	Sjostrom et al. (2006)
01DS102	42.4446	-107.5588	14.2	12.7		-110		43.1	Sjostrom et al. (2006)
01DS103	42.4350	-107.5628	14.2	12.8		-118		38.3	Sjostrom et al. (2006)
01DS116	42.7288	-107.5826	14.2	12.8		-112		41.5	Sjostrom et al. (2006)
01DS115	42.7308	-107.5845	14.2	11.9		-113		45.0	Sjostrom et al. (2006)
01DS121	42.6817	-108.1239	14.2	14.5		-116		32.3	Sjostrom et al. (2006)
01DS34	42.7154	-103.8828	19.2	16.8		-95		33.6	Sjostrom et al. (2006)
01DS37	42.4373	-103.4184	21.9	19.7		-127		8.8	Sjostrom et al. (2006)
01DS36	42.4271	-103.5419	21.9	16.2		-121		23.3	Sjostrom et al. (2006)
01DS35	42.4234	-103.7525	21.9	15.0		-94		41.7	Sjostrom et al. (2006)
01DS28	42.7690	-103.5354	22	18.8		-93		26.7	Sjostrom et al. (2006)
01DS44	42.9492	-103.6854	22	18.8		-97		24.8	Sjostrom et al. (2006)
01DS33	42.7425	-103.8113	22	16.7		-93		35.0	Sjostrom et al. (2006)
01DS31	42.7791	-103.5321	30.3	17.2		-93		33.0	Sjostrom et al. (2006)
01DS30	42.7688	-103.5835	30.3	16.8		-107		27.6	Sjostrom et al. (2006)
01DS12	41.5968	-103.1131	31.25	18.3		-94		28.1	Sjostrom et al. (2006)
01DS14	41.5968	-103.1131	31.25	18.0		-88		32.3	Sjostrom et al. (2006)
01DS15	41.5968	-103.1131	31.25	18.0		-92		30.3	Sjostrom et al. (2006)
01DS16	41.5968	-103.1131	31.25	20.2		-110		14.1	Sjostrom et al. (2006)
01DS17	41.5968	-103.1131	31.25	17.6		-102		27.0	Sjostrom et al. (2006)
01DS18	41.5968	-103.1131	31.25	17.3		-123		18.5	Sjostrom et al. (2006)
01DS19	41.6991	-103.3415	31.25	19.2		-100		22.0	Sjostrom et al. (2006)
01DS20	41.6991	-103.3415	31.25	18.6		-90		28.9	Sjostrom et al. (2006)
01DS84	42.7125	-105.3710	31.25	14.7		-112		33.5	Sjostrom et al. (2006)
01DS113	42.7574	-107.5635	32	10.9		-126		42.2	Sjostrom et al. (2006)
01DS129	42.5848	-108.2870	32	10.6		-104		56.6	Sjostrom et al. (2006)
01DS39	42.9194	-103.4913	34.5	16.9		-123		19.9	Sjostrom et al. (2006)

**Table 1** (continued)

Sample	Latitude	Longitude	Age (Ma)	$\delta^{18}\text{O}$	$1\sigma$	$\delta\text{D}$	$1\sigma$	Temperature (°C)	Key references
01DS55	42.8288	-101.6981	35	17.7	-107	24.2		Sjostrom et al. (2006)	
01DS69	42.8630	-101.8605	35.5	18.6	-103	22.8		Sjostrom et al. (2006)	
01DS72	43.8614	-102.8631	35.5	18.4	-101	24.4		Sjostrom et al. (2006)	
01DS74	43.8614	-102.8631	35.5	20.0	-101	18.7		Sjostrom et al. (2006)	
01DS81	42.7625	-105.0128	35.5	16.6	-101	31.4		Sjostrom et al. (2006)	
01DS89	42.6386	-106.7545	35.65	13.9	-107	39.5		Sjostrom et al. (2006)	
01DS90a	42.6386	-106.7545	35.65	15.5	-122	25.5		Sjostrom et al. (2006)	
01DS91	42.6386	-106.7545	35.65	14.4	-118	31.7		Sjostrom et al. (2006)	
01DS92	42.6386	-106.7545	35.65	14.2	-109	37.1		Sjostrom et al. (2006)	
01DS93	42.6386	-106.7545	35.65	14.1	-122	30.9		Sjostrom et al. (2006)	
01DS94	42.6386	-106.7594	35.65	13.9	-121	32.2		Sjostrom et al. (2006)	
01DS95	42.6386	-106.7594	35.65	13.7	-124	31.5		Sjostrom et al. (2006)	
01DS97	42.6386	-106.7594	35.65	14.3	-117	32.6		Sjostrom et al. (2006)	
01DS98	42.6390	-106.7650	35.65	13.4	-126	31.7		Sjostrom et al. (2006)	
01DS99	42.6390	-106.7650	35.65	14.3	-124	29.1		Sjostrom et al. (2006)	
01DS100	42.6390	-106.7650	35.65	13.6	-120	33.9		Sjostrom et al. (2006)	
01DS101	42.6390	-106.7650	35.65	14.0	-113	35.9		Sjostrom et al. (2006)	
01DS75	43.8608	-102.8636	37	19.6	-99	21.0		Sjostrom et al. (2006)	
01DS110	42.7575	-107.5874	49	13.6	-122	32.9		Sjostrom et al. (2006)	
01DS111	42.7608	-107.5900	49	14.7	-122	28.5		Sjostrom et al. (2006)	
01DS123	42.7091	-108.1809	49	16.1	-107	30.4		Sjostrom et al. (2006)	
01DS124	42.7091	-108.1809	49	12.7	-101	48.2		Sjostrom et al. (2006)	
01DS128	42.5964	-108.2933	49	15.7	-113	29.0		Sjostrom et al. (2006)	
Mean	42.5733	-105.3373		15.8	-109.2	30.9			
<i>Trapper Creek, ID (Horton et al., 2004)</i>									
TC-LTC-2	42.1250	-114.0000	10.25	14.1	-112	36.0		Horton et al. (2004)	
TC-1H-6	42.1250	-114.0000	11.6	12.3	-113	43.2		Horton et al. (2004)	
TC-1H-5	42.1250	-114.0000	11.81	12.6	-114	41.3		Horton et al. (2004)	
TC-1H-3	42.1250	-114.0000	12.3	11.8	-115	44.3		Horton et al. (2004)	
TC-1H-1	42.1250	-114.0000	12.82	8.5	-147	41.2		Horton et al. (2004)	
TC-VH-6	42.1250	-114.0000	12.82	10.6	-123	45.2		Horton et al. (2004)	
TC-VH-5	42.1250	-114.0000	12.9	9.8	-118	51.9		Horton et al. (2004)	
TC-VH-4	42.1250	-114.0000	13.1	9.8	-127	46.6		Horton et al. (2004)	
TC-VH-3	42.1250	-114.0000	13.4	11.0	-128	40.6		Horton et al. (2004)	
TC-VH-2	42.1250	-114.0000	13.5	10.7	-129	41.4		Horton et al. (2004)	
Mean	42.1250	-114.0000		11.1	-122.6	43.2			
<i>El Paso Basin, CA (Horton and Chamberlain, 2006)</i>									
EPB-7	35.4333	-117.9267	7.0	21.0	-102	14.8		Horton and Chamberlain (2006)	
EPB-6	35.4333	-117.9267	8.9	20.9	-105	13.9		Horton and Chamberlain (2006)	
EPB-3	35.4333	-117.9267	9.8	18.5	-102	23.6		Horton and Chamberlain (2006)	
EPB-13	35.4333	-117.9267	12.5	14.8	-110	34.1		Horton and Chamberlain (2006)	
EPB-11	35.4333	-117.9267	13.0	15.8	-106	32.1		Horton and Chamberlain (2006)	
EPB-10	35.4333	-117.9267	13.2	13.6	-111	38.6		Horton and Chamberlain (2006)	
EPB-9	35.4333	-117.9267	13.5	15.9	-111	29.2		Horton and Chamberlain (2006)	
Mean	35.4333	-117.9267		17.2	-106.7	26.6			
<i>Rainbow Basin (CA (Horton and Chamberlain, 2006)</i>									
MD/CA-11	35.0223	-117.0346	2.1	19.1	-102	21.4		Horton and Chamberlain (2006)	
MD/CA-07	35.0223	-117.0346	14.8	17.2	-103	28.0		Horton and Chamberlain (2006)	
BF-36	35.0223	-117.0346	15.2	18.6	-104	22.3		Horton and Chamberlain (2006)	
BF-24	35.0223	-117.0346	15.8	16.4	-110	27.7		Horton and Chamberlain (2006)	
BF-05	35.0223	-117.0346	19.3	15.6	-99	36.5		Horton and Chamberlain (2006)	
MD/CA-20	35.0223	-117.0346	19.7	19.2	-96	23.8		Horton and Chamberlain (2006)	
Mean	35.0223	-117.0346		17.7	-102.3	26.6			

ern flank of the Rocky Mountains (2.3). We interpret these to represent high ancient LMWL slopes, which are roughly in agreement with modern LMWLs in western North America (Kendall and Coplen, 2001). Their location to the north and east of the Basin and Range sup-

ports the hypothesis that change in the hydrologic cycle may be the driver of smectite isotopic composition in these basins. In the case of the eastern flank of the Rocky Mountains,  $\delta^{18}\text{O}$  decreases from the Eocene to the Miocene, and records the interaction of airmasses and high

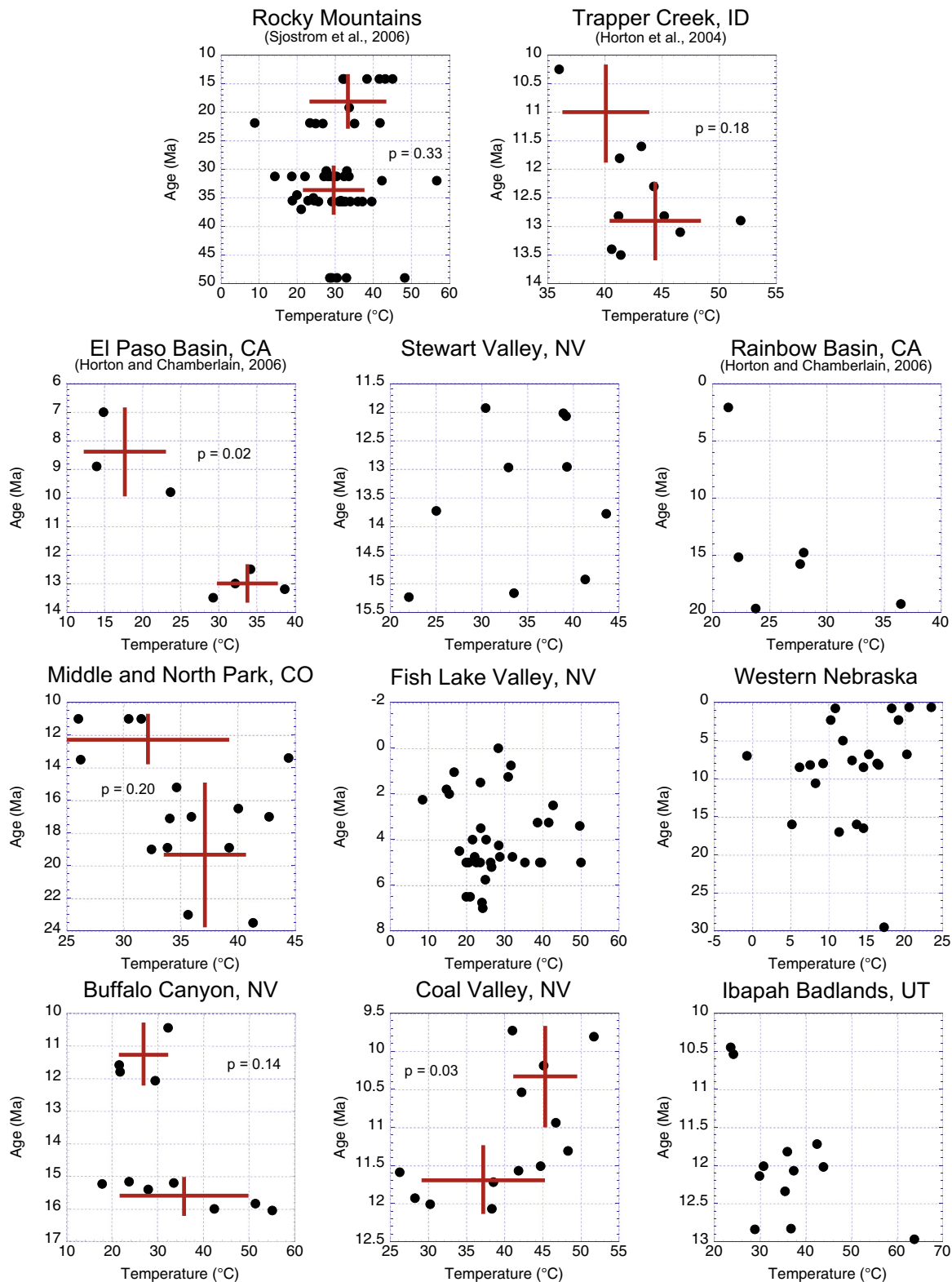


Fig. 4. Smectite formation temperature vs. age for Cenozoic basins in western North America. Red crosses indicate age range, mean and  $1\sigma$  variation for binned samples in selected basins. *p* Values correspond to two-tailed *t*-tests of binned samples. (For interpretation of the references to color in this figure legend, the reader is referred to the web version of this article.)

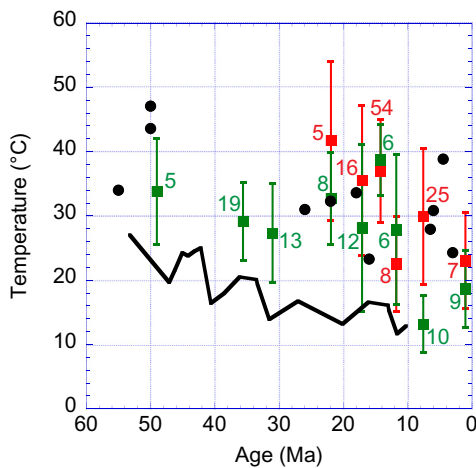


Fig. 5. Comparison of terrestrial paleotemperature estimates in Cenozoic western North America. Black line represents data from mid-latitude paleofloral assemblages (Wolfe, 1994), black circles are from carbonate clumped isotope data (Huntington et al., 2010 and Snell et al., 2013). Smectite data are squares with  $1\sigma$  error bars (Green are from Rocky Mountains and Great Plains, Red are from the Basin and Range). Numbers next to smectite geothermometry data indicate the number of samples in each bin. (For interpretation of the references to color in this figure legend, the reader is referred to the web version of this article.)

topography in the Rocky Mountains (Sjostrom et al., 2006). Here and in Miocene Trapper Creek, ID, the high smectite line slope confirms the hypothesis that changing meteoric water composition is the primary control on smectite composition, supporting prior interpretations that topographic development affected atmospheric circulation.

Within the Basin and Range, all basins sampled indicate a low or negative smectite line slope. The three northernmost sections in the Basin and Range (Buffalo Canyon and Coal Valley, NV, and the Ibapah Badlands, UT) all exhibit a negative slope in the smectite line. Taken at face value, these slopes cannot be produced by meteoric waters and evaporation, and require, at least in part, changing temperature of smectite formation. Therefore, we interpret the negative slopes as indicative of change in temperature as the primary control on smectite isotopic composition in the Miocene northern Basin and Range.

The four additional Basin and Range sections (Miocene to Pleistocene Fish Lake Valley, NV, Middle to Late Miocene El Paso Basin, CA, Middle Miocene Stewart Valley, NV, and Early Miocene to Pleistocene Rainbow Basin, CA) as well as Early to Middle Miocene Middle and North Park, CO and Oligocene to Pleistocene Nebraska exhibit shallow smectite line slopes of 0–2. In this intermediate range, assigning a single underlying cause as the control of smectite isotopic composition is more challenging. These low slopes could be caused by a combination of changing water composition and temperature change, as well as evaporative enrichment of surface waters.

We present several first-order interpretations from this  $\delta^{18}\text{O}$ – $\delta\text{D}$  smectite record. First, smectite line slopes indicate

that changes in meteoric water composition due to changes in moisture source, trajectory or vapor recycling are the primary cause of isotopic change outside the Basin and Range. Within the Northern and Central Basin and Range, negative slopes suggest that changes in mineral formation temperature outweigh changes in surface water composition. Finally, within the Southern and Western Basin and Range, Great Plains, and eastern flank of the Rocky Mountains intermediate slopes in the smectite line suggest a combination of causes including aridification as responsible for changes in the smectite record. Finally, it is important to recognize the limitations of such records. These records represent the combined effects of changing temperature and evolved surface water composition over millions of years.

## 5.2. Interpretation of smectite paleotemperature record

The composite temperature records in the Rocky Mountains and Great Plains as well as the Basin and Range match prevailing global climate trends to a first order. In the Basin and Range, temperatures steadily decrease since the Early to Middle Miocene by over 15 °C. This is of a substantially greater magnitude than evidenced in marine records, as global mean temperatures during the Middle Miocene were approximately 3 °C warmer than today (You et al., 2009). Our Cenozoic smectite temperature cooling trend, however, is consistent with paleofloral records from the continental interior, which exhibit a high degree of spatial and temporal variability in temperature during the Neogene (Wolfe, 1994; Wolfe et al., 1997; Chase et al., 1998). In the Rocky Mountains and Great Plains record, Paleogene and Early Miocene temperatures are also warm, ranging between 10 and 15 °C greater than samples from the Late Miocene and Pliocene. The highest recorded temperature of 39 °C from the Rocky Mountains and Great Plains occurs during the Middle Miocene.

This smectite paleotemperature record is a meaningful addition to existing paleofloral and carbonate clumped isotope estimates of terrestrial temperatures in western North America. Leaf margin analysis from paleofloral data has produced estimates ranging between 9 and 17 °C in Miocene California, Nevada, Oregon and Washington (Wolfe et al., 1997; Chase et al., 1998). These temperature estimates are much closer to modern mean annual air temperatures in western North America. Estimates from carbonate-based thermometry are substantially higher. For example, clumped isotope data from the Colorado Plateau from the Middle Miocene to Pliocene are greater than 28 °C on average (Huntington et al., 2010). Clumped isotope temperature estimates of the Paleocene–Eocene Bighorn Basin, WY are ~34 °C (Snell et al., 2013). Similarly, the smectite geothermometry record in this study produces temperatures well in excess of 20 °C during most of the Neogene. Two-tailed heteroscedastic  $t$ -tests indicate that geochemical estimates of temperature in the Neogene Basin and Range and Colorado Plateau are significantly higher than paleofloral estimates (Smectite vs. Paleofloral  $p = 4.6 \times 10^{-15}$ , Clumped vs. Paleofloral  $p = 1.1 \times 10^{-4}$ ). Populations of Neogene smectite and clumped isotope temperatures do not vary significantly ( $p = 0.15$ ).

There may be some common reasons for the systematic disparity between paleofloral and geochemical estimates of temperature. First, geochemical records may be subject to biases in seasonality or specific conditions of formation. Clay minerals may have some advantages over carbonates as they are less likely to undergo rapid growth during brief periods of extremely warm or evaporitic conditions. Clumped isotope records have been demonstrated to reflect summer temperatures as opposed to mean annual air temperature (Breecker et al., 2009; Quade et al., 2013; Snell et al., 2013).

There is the possibility that some of the smectite paleotemperature record may reflect high crustal heat flow, particularly those from the Basin and Range. Even though samples may not have been subjected to great depth, regions such as the Basin and Range have elevated geothermal gradients that could potentially affect the temperature of mineral formation (see Section 5.3). In particular, basins in close proximity to the Miocene-Quaternary Yellowstone hotspot track or other volcanic sources could reflect local or regional changes in heat flow. While we acknowledge this possibility, the stratigraphic sections sampled in this work did not show signs of high-temperature alteration or diagenesis such as illite-smectite mixed layering. In addition, smectite-based temperatures do not exhibit systematically higher temperatures in the Basin and Range or adjacent to the Yellowstone hotspot track than in other regions such as the Rocky Mountains or Great Plains. Furthermore, the calculated smectite temperatures produced here are in accordance with published clumped isotope data in carbonates reflecting Cenozoic summer soil temperatures.

Finally, the method of Delgado and Reyes (1996) shows promise for terrestrial paleoclimate applications but improvements are necessary if smectite geothermometry is to be a leading paleotemperature metric. We suggest three major considerations for future application and refinement of this technique. First, the clay minerals studied must be well-characterized as differences in stoichiometry and mineralogy affect isotopic fractionation (see Section 5.3). Second, the fractionation factors used here have not necessarily been well calibrated for low temperatures and near-surface environments. Lastly, additional experimental studies of hydrogen isotope exchange would be particularly valuable in improving phyllosilicate-based geothermometry.

### 5.3. Phyllosilicate formation, composition and other confounding effects

In order to confidently assert that surface processes such as climatic change are the primary control on the smectite record, we must demonstrate that smectite formation occurred near the surface soon after deposition of the sediments. Multiple studies indicate that smectite forms readily in the shallow subsurface. For example, strontium isotopic and petrographic studies of the Neogene Arikaree and Ogallala Groups sampled in this study from Nebraska indicate that the authigenic smectite formed soon after deposition (Stanley and Benson, 1979; Stanley and Faure, 1979).

In addition, authigenic smectite is found in Quaternary soils and moraines, and ash from the 1980 Mount Saint Helens eruption has since converted to clay minerals in many locations (Sjostrom et al., 2006 and references therein).

Several lines of evidence suggest that our samples formed in the shallow subsurface. First, most samples were collected in poorly consolidated air fall ashes and paleosols from shallow basins. Indurated ashes that may have been subjected to higher temperatures and/or diagenetic alteration rarely yielded enough clay-sized fraction for isotopic analysis. As such, the samples we analyzed are nearly all poorly consolidated and unlikely reflect deep burial. Second, smectite begins converting to illite at temperatures over 35 °C, with the majority of conversion occurring between 55 and 95 °C (Perry and Hower, 1970). X-ray diffraction analysis confirmed the composition of our samples to be primarily smectite, further supporting a shallow depth of formation. The stratigraphic sections sampled in this study were under 1 km in thickness. Typical geothermal gradients in modern western North America mostly vary between 25 and 40 °C/km (e.g., Blackwell, 1983; Law et al., 1989), although more elevated gradients are observed in locations such as the modern Yellowstone hotspot track. Given a geothermal gradient of 25–40 °C/km, however, we would expect phyllosilicates to undergo some illitization by 1 km in depth, which is not evident from our X-ray diffraction analysis. As such, we argue that the isotopic signatures of the phyllosilicates presented in this study likely reflect little alteration or isotopic exchange and preserve the isotopic signature of the near surface environment in which the minerals formed. In addition, because we sampled airfall ashes that show no evidence of reworking, we rule out the potential for detrital minerals to be incorporated into the samples we analyzed.

Variations in the mole fraction of Al, Fe and Mg in the octahedral layer of 2:1 phyllosilicates can affect mineral-water isotope equilibrium fractionation factors (Savin and Lee, 1988; Gilg and Sheppard, 1996). Due to the relative lack of existing isotope data for well-characterized phyllosilicates, we compared two approaches for the smectite-water hydrogen isotope fractionation factor. The first, shown in our tables and figures here, utilizes the fractionation factor of Capuano (1992) and follows the temperature derivation of Delgado and Reyes (1996). In order to account for variations in phyllosilicate elemental composition, we incorporated composition data for several samples (Supp. Table 1) and calculated temperatures following a bond-model approximation (e.g., Savin and Lee, 1988; Tabor and Montañez, 2005; Rosenau and Tabor, 2013). The bond-model calculations yield mineral-formation temperatures that are ~3 to 4 °C cooler than the temperatures calculated using the traditional Capuano (1992) approach (Supp. Table 2). One particularly Fe-rich sample (HM08-CV7) however, produces a calculated temperature 7 °C warmer than the Capuano (1992) fractionation factor (Supp. Table 2). These results indicate that differences up to several °C in calculated mineral formation temperature are possible due to changes in phyllosilicate composition. Given the spatial and temporal breadth of our samples and the relative similarity among the temperatures

calculated via these two approaches, we continue to interpret the first-order trends in temperature in the context of paleoclimatic conditions. While we lack elemental composition data for nearly all of our samples, substantial and systematic decreases in octahedral Fe content among samples across western North America would be required to produce the observed 10–15 °C decrease in smectite temperatures since the Middle Miocene. Nonetheless, variation in phyllosilicate composition cannot be ruled out as a possible source of change in calculated temperature and is yet another source of complexity for this geothermometry approach.

## 6. CONCLUSION

We conclude that the smectite records presented here are consistent with prior interpretations of paleoclimatic change in western North America. Our assessment of meteoric water relationships in western North America matches patterns existing in the modern. Basins exhibiting steep ancient meteoric water line slopes occur in present day Idaho, Nebraska and South Dakota, while those with shallow inferred ancient meteoric water line slopes exist within the arid, inwardly-drained Basin and Range. The smectite paleotemperature record is congruent with deep-ocean temperature records to a first order. Composite temperature records from the Basin and Range as well as the Rocky Mountains and Great Plains indicate cooling on the order of 10–15 °C since the Middle Miocene Climatic Optimum. We argue that the exaggerated nature of this shift in comparison to the marine record is indicative of continentality and is consistent with existing geochemical estimates from carbonate in Cenozoic western North America.

## ACKNOWLEDGEMENTS

We acknowledge Scott Jasechko and two anonymous reviewers for their encouragement and constructive reviews. We thank Peter Blisniuk, Walter Torres, Arturas Vailionis and the Washington State University GeoAnalytical Lab for laboratory assistance. This research was supported by National Science Foundation Grants EAR-0609649 and EAR-1019648.

## APPENDIX A. SUPPLEMENTARY DATA

Supplementary data associated with this article can be found, in the online version, at <http://dx.doi.org/10.1016/j.gca.2014.07.008>.

## REFERENCES

- Abruzzese M., Waldbauer J. and Chamberlain C. P. (2005) Oxygen and hydrogen isotope ratios in freshwater chert as indicators of ancient climate and hydrologic regime. *Geochim. Cosmochim. Acta* **69**, 1377–1390.
- Axelrod D. I. (1991) *The Early Miocene Buffalo Canyon flora of western Nevada*. The University of California Press, Berkeley.
- Beckley A. L. (1915) Geology and coal resources of North Park, Colorado. *U.S. Geol. Surv. Bull.* **596**.
- Blackwell D. D. (1983) *Heat flow in the northern Basin and Range province. The Role of Heat in the Development of Energy and Mineral Resources in the Northern Basin and Range Province*. Special Report 13. Geothermal Resources Council, pp. 81–93.
- Boellstorff J. (1976) The succession of late Cenozoic volcanic ashes in the Great Plains; a progress report. *Guidebook Series – Kansas Geological Survey*, pp. 37–71.
- Breecker D. O., Sharp Z. D. and McFadden L. D. (2009) Seasonal bias in the formation and stable isotopic composition of pedogenic carbonate in modern soils from central New Mexico, USA. *Geol. Soc. Am. Bull.* **121**, 630–640.
- Capuano R. M. (1992) The temperature dependence of hydrogen isotope fractionation between clay minerals and water: evidence from a geopressurized system. *Geochim. Cosmochim. Acta* **56**, 2547–2554.
- Chamberlain C. P. and Poage M. A. (2000) Reconstructing the paleotopography of mountain belts from the isotopic composition of authigenic minerals. *Geology* **28**, 115–118.
- Chase C. G., Gregory-Wodzicki K. M., Parrish-Jones J. T. and DeCelles P. G. (1998) Topographic history of the western Cordillera of North America and controls on climate. In *Tectonic Boundary Conditions for Climate Model Simulations* (eds. T. J. Crowley and K. Burke). Oxford University Press, New York, pp. 73–99.
- Clark I. D. and Fritz P. (1997) *Environmental Isotopes in Hydrogeology*. Lewis Publishers.
- Craig H. (1961) Isotopic variations in meteoric waters. *Science* **133**, 1702–1703.
- Craig H. and Gordon L. I. (1965) *Deuterium and Oxygen 18 Variations in the Ocean and the Marine Atmosphere*. Consiglio nazionale delle ricerche, Laboratorio di geologia nucleare.
- Dansgaard W. (1964) Stable isotopes in precipitation. *Tellus* **16**.
- Delgado A. and Reyes E. (1996) Oxygen and hydrogen isotope compositions in clay minerals: a potential single-mineral geothermometer. *Geochim. Cosmochim. Acta* **60**, 4285–4289.
- Diffendal R. (1995) Geology of the Ogallala/High Plains regional aquifer system in Nebraska; Field trip No. 6. *Guidebook*. University of Nebraska-Lincoln, Conservation and Survey Division **10**, pp. 61–75.
- Friedman I. (1953) Deuterium content of natural waters and other substances. *Geochim. Cosmochim. Acta* **4**, 89–103.
- Gilg H. A. and Sheppard S. M. F. (1996) Hydrogen isotope fractionation between kaolinite and water revisited. *Geochim. Cosmochim. Acta* **60**, 529–533.
- Golia R. T. and Stewart J. H. (1984) Depositional environments and paleogeography of the Upper Miocene Wassuk Group, west-central Nevada. *Sed. Geol.* **38**, 159–180.
- Heylman E. B. (1965) Reconnaissance of the tertiary sedimentary rocks in western Utah. *Utah Geol. Mineral. Surv. Bull.* **75**, 38.
- Horton T. W. and Chamberlain C. P. (2006) Stable isotopic evidence for Neogene surface downdrop in the central Basin and Range province. *Geol. Soc. Am. Bull.* **118**, 475–490.
- Horton T. W., Sjostrom D. J., Abruzzese M. J., Poage M. A., Waldbauer J. R., Hren M., Wooden J. and Chamberlain C. P. (2004) Spatial and temporal variation of Cenozoic surface elevation in the Great Basin and Sierra Nevada. *Am. J. Sci.* **304**, 862–888.
- Huntington K. W., Eiler J. M., Affek H. P., Guo W., Bonifacie M., Yeung L. Y., Thiagarajan N., Passey B., Tripati A., Daeron M. and Came R. (2009) Methods and limitations of “clumped” CO<sub>2</sub> isotope ( $\Delta_{47}$ ) analysis by gas-source isotope ratio mass spectrometry. *J. Mass Spectrom.* **44**, 1318–1329.
- Huntington K. W., Wernicke B. P. and Eiler J. M. (2010) Influence of climate change and uplift on Colorado Plateau paleotemperatures from carbonate clumped isotope thermometry. *Tectonics* **29**, TC3005.

- Izett G. (1968) Geology of the Hot Sulphur Springs Quadrangle, Grand County, Colorado. *U.S. Geological Survey Professional Paper* 79.
- Izett, G. and Barclay, C. (1973). Geologic map of the Kremmling Quadrangle, Grand County, Colorado. *Geologic Quadrangle Map*, U.S. Geological Survey.
- Johnson D. M., Hooper P. R. and Conrey R. M. (1999) XRF analysis of rocks and minerals for major and trace elements on a single low dilution Li-tetraborate fused bead. *Adv. X-Ray Anal.* **41**, 843–867.
- Kendall C. and Coplen T. B. (2001) Distribution of oxygen-18 and deuterium in river waters across the United States. *Hydro. Process.* **15**, 1363–1393.
- Kohn M. J., Miselis J. L. and Fremd T. J. (2002) Oxygen isotope evidence for progressive uplift of the Cascade Range. *Earth Planet. Sci. Lett.* **204**, 151–165.
- Law B. E., Spencer C. W., Charpentier R. R. Crovelli, R. A., Mast R. F., Dolton G. L. and Wandrey C. J. (1989) Estimates of gas resources in overpressured low-permeability Cretaceous and Tertiary sandstone reservoirs, Greater Green River Basin, Wyoming, Colorado and Utah. In *Gas Resources of Wyoming: Wyoming Geological Association Fortieth Field Conference Guidebook* (ed. J. L. Eisert), pp. 39–61.
- Lawrence J. R. and Taylor H. P. (1971) Deuterium and O-18 correlation – clay minerals and hydroxides in quaternary soils compared to meteoric waters. *Geochim. Cosmochim. Acta* **35**, 993–1003.
- Lawrence J. R. and Taylor H. P. (1972) Hydrogen and oxygen isotope systematics in weathering profiles. *Geochim. Cosmochim. Acta* **36**, 1377–1393.
- Mix H. T., Mulch A., Kent-Corson M. L. and Chamberlain C. P. (2011) Cenozoic migration of topography in the North American Cordillera. *Geology* **39**, 87–90.
- Mix H. T., Winnick M. J., Mulch A. and Chamberlain C. P. (2013) Grassland expansion as an instrument of hydrologic change in Neogene western North America. *Earth Planet. Sci. Lett.* **377–378**, 73–83.
- Montague J. (1991) Cenozoic history of the Saratoga Valley area, Wyoming and Colorado. *Rocky Mt. Geol.* **29**, 13–70.
- Montague J. de I and Barnes W. C. (1957) Stratigraphy of the North Park Formation, in the North Park Area, Colorado. In *Guidebook to the Geology of North and Middle Park Basins, Colorado*. Rocky Mountain Association of Geologists, pp. 55–60.
- Moore D. M. and Reynolds, Jr. R. C. (1997) *X-Ray Diffraction and the Identification and Analysis of Clay Minerals*, second ed. Oxford University Press, New York.
- Mulch A., Graham S. A. and Chamberlain C. P. (2006) Hydrogen isotopes in Eocene river gravels and paleoelevation of the Sierra Nevada. *Science* **313**, 87–89.
- Mulch A., Teyssier C., Cosca M. A. and Chamberlain C. P. (2007) Stable isotope paleoaltimetry of Eocene core complexes in the North American Cordillera. *Tectonics* **26**, TC4001.
- Mulch A., Sarna-Wojcicki A. M., Perkins M. E. and Chamberlain C. P. (2008) A Miocene to Pleistocene climate and elevation record of the Sierra Nevada (California). *Proc. Natl. Acad. Sci. USA* **105**, 6819–6824.
- Muttik N., Kirsimäe K. and Vennemann T. W. (2010) Stable isotope composition of smectite in suevites at the Ries crater, Germany: implications for hydrous alteration of impactites. *Earth Planet. Sci. Lett.* **299**, 190–195.
- Myers T. S., Tabor N. J. and Jacobs L. L. (2011) Late Jurassic paleoclimate of Central Africa. *Palaeogeogr. Palaeoclimatol. Palaeoecol.* **311**, 111–125.
- Perkins M. E., Brown F. H., Nash W. P., McIntosh W. and Williams S. K. (1998) Sequence, age, and source of silicic fallout tuffs in middle to late Miocene basins of the northern Basin and Range province. *Geol. Soc. Am. Bull.* **110**, 344–360.
- Perry E. D. and Hower J. (1970) Burial diagenesis in Gulf Coast pelitic sediments. *Clays Clay Miner.* **18**, 165–177.
- Poage M. A. and Chamberlain C. P. (2002) Stable isotopic evidence for a Pre-Middle Miocene rain shadow in the western Basin and Range: implications for the paleotopography of the Sierra Nevada. *Tectonics* **21**. <http://dx.doi.org/10.1029/2001TC001303>.
- Quade J., Eiler J., Daëron M. and Achyuthan H. (2013) The clumped isotope geothermometer in soil and paleosol carbonate. *Geochim. Cosmochim. Acta* **105**, 92.
- Reheis M. C. and Sawyer T. L. (1997) Late Cenozoic history and slip rates of the Fish Lake Valley, Emigrant Peak, and Deep Springs fault zones, Nevada and California. *Geol. Soc. Am. Bull.* **109**, 280–299.
- Reheis M.C. and Block D. (2007) Surficial geologic map and geochronologic database, Fish Lake Valley, Esmeralda County, Nevada, and Mono County, California. *U.S. Geological Survey Data Series* 277.
- Rosenau N. A. and Tabor N. J. (2013) Oxygen and hydrogen isotope compositions of paleosol phyllosilicates: differential burial histories and determination of Middle-Late Pennsylvanian low-latitude terrestrial paleotemperatures. *Palaeogeogr. Palaeoclimatol. Palaeoecol.* **392**, 382–397.
- Rozanski K., Araguas-Araguas L., Gonfiantini R., Swart P. K., Lohwan K. L., McKenzie J. A. and Savine S. (1993) Isotopic patterns in modern global precipitation. In *Climate Change in Continental Isotopic Records*. American Geophysical Union, Washington, DC, pp. 1–37.
- Savin S. M. and Lee M. (1988) Isotopic studies of phyllosilicates. *Rev. Mineral.* **19**, 189–223.
- Sharp Z. D. (1990) A laser-based microanalytical method for the in situ determination of oxygen isotope ratios of silicates and oxides. *Geochim. Cosmochim. Acta* **54**, 1353–1357.
- Sheppard S. M. F. and Gilg H. A. (1996) Stable isotope geochemistry of clay minerals. *Clay Miner.* **31**, 1–24.
- Schorn H. E., Scudder H. I., Savage D. E. and Firby J. R. (1989) General stratigraphy and paleontology of the Miocene continental sequence in Stewart Valley, Mineral County, Nevada, USA. In *Proceedings of International Symposium of Pacific Neogene Continental and Marine Events, National Working Group of China for IGCP-246* (eds. Li Gengwu, Tsuchi Ryuichi and Li Qibin). Nanjing University Press, Nanjing, China, pp. 157–173.
- Sjostrom D. J., Hren M., Horton T. W., Waldbauer J. R. and Chamberlain C.P. (2006) Stable isotopic evidence for a pre-late Miocene elevation gradient in the Great Plains – Rocky Mountain Region, USA. *GSA Special Papers* **398**, 309–319.
- Snell K. E., Thrasher B. L., Eiler J. M., Koch P. L., Sloan L. C. and Tabor N. J. (2013) Hot summers in the Bighorn Basin during the early Paleogene. *Geology* **41**, 55–58.
- Stanley K.O. and Benson L. V. (1979) Early diagenesis of High Plains Tertiary citric and arkosic sandstone, Wyoming and Nebraska. In *Aspects of Diagenesis* (eds. P. A. Scholle and P. R. Schluger). Society of Economic Paleontologists and Mineralogists Special Publication 26, pp. 401–423.
- Stanley K. O. and Faure G. (1979) Isotopic composition and sources of strontium in sandstone cements – high-plains sequence of Wyoming and Nebraska. *J. Sediment. Petrol.* **49**, 45–53.
- Stern L. A., Chamberlain C. P., Reynolds R. C. and Johnson G. D. (1997) Oxygen isotope evidence of climate change from pedogenic clay minerals in the Himalayan molasse. *Geochim. Cosmochim. Acta* **61**, 731–744.

- Stout T., DeGraw H., Tanner L., Stanley K., Wayne W. and Swinehart J. (1971) Guidebook to the Late Pliocene and Early Pleistocene of Nebraska. Nebr. Geol. Surv., Lincoln, NE.
- Swineford A., Frye J. and Leonard A. (1955) Petrography of the late Tertiary volcanic ash falls in the central Great Plains [Kansas-Nebraska]. *J. Sediment. Petrol.* **25**, 243–261.
- Swinehart J., Souders V., DeGraw H. and Diffendal R. (1985) *Cenozoic Paleogeography of western Nebraska*. Rocky Mt. Sect., Soc. Econ. Paleontol. and Mineral., Denver, CO, pp. 209–229.
- Tabor N. J. and Montañez I. P. (2005) Oxygen and hydrogen isotope compositions of Permian pedogenic phyllosilicates: development of modern surface domain arrays and implications for paleotemperature reconstructions. *Palaeogeogr. Palaeoclimatol. Palaeoecol.* **223**, 127–146.
- Tabor N. J., Montañez I. P., Zierenberg R. and Currie B. S. (2004) Mineralogical and geochemical evolution of a basalt-hosted fossil soil (Late Triassic, Ischigualasto Formation, northwest Argentina): potential for paleoenvironmental reconstruction. *Geol. Soc. Am. Bull.* **116**, 1280–1293.
- Takeuchi A. and Larson P. B. (2005) Oxygen isotope evidence for the late Cenozoic development of an orographic rain shadow in eastern Washington, USA. *Geology* **33**, 313–316.
- Vitali F., Longstaffe F. J., McCarthy P. J., Plint A. G. and Caldwell W. G. E. (2002) Stable isotopic investigation of clay minerals and pedogenesis in an interfluvial paleosol from the Cenomanian Dunvegan Formation, N.E. British Columbia, Canada. *Chem. Geol.* **192**, 269–287.
- Wolfe J. A. (1994) Tertiary climatic changes at middle latitudes of western North America. *Palaeogeogr. Palaeoclimatol. Palaeoecol.* **108**, 195–205.
- Wolfe J. A., Schorn H. E., Forest C. E. and Molnar P. (1997) Paleobotanical evidence for high altitudes in Nevada during the Miocene. *Science* **276**, 1672–1675.
- Yapp C. J. (1987) Oxygen and hydrogen isotope variations among goethites ( $\alpha$ -FeOOH) and the determination of paleotemperatures. *Geochim. Cosmochim. Acta* **51**, 355–364.
- Yeh H. W. (1980) D/H ratios and late-stage dehydration of shales during burial. *Geochim. Cosmochim. Acta* **44**, 341–352.
- Yeh H. W. and Epstein S. (1978) Hydrogen isotope exchange between clay-minerals and sea-water. *Geochim. Cosmochim. Acta* **42**, 140–143.
- You Y., Huber M., Müller R. D., Poulsen C. J. and Ribbe J. (2009) Simulation of the middle Miocene climate optimum. *Geophys. Res. Lett.* **36**, L04702.
- Yurtsever Y. and Gat J. R. (1981) Atmospheric waters. In *Stable Isotope Hydrology: Deuterium and Oxygen-18 in the Water Cycle*. IAEA Technical Report Series 210, pp. 103–142.

Associate editor: Annie B. Kersting